J. Appl. Comput. Mech., 12(4) (2026) 1650-1666
DOI: 10.22055/jacm.2026.49360.5917

ISSN: 2383-4536
jacm.scu.ac.ir

Shahid Chamran University of Ahvaz

Journal of Applied and Computational Mechanics

Research Paper

Dynamic Fractional-Order Computational Modeling of Lung Cancer: A Hybrid Biomechanical–Therapy Framework

Shubham Ashok Ambhore[1], Navneet Kumar Lamba[2]

[1] Research Scholar, Post Graduate Teaching Department of Mathematics, Rashtrasant Tukadoji Maharaj Nagpur University, Nagpur, Maharashtra, India, Email: shubham.ambhoremaths@gmail.com

[2] Department of Mathematics, Shri Lemdeo Patil Mahavidyalaya, Mandhal, Rashtrasant Tukadoji Maharaj Nagpur University, Nagpur, Maharashtra, India, Email: navneetkumarlamba@gmail.com

Received May 10 2026; Revised July 02 2026; Accepted for publication July 04 2026.
✉ Corresponding author: N.K. Lamba (navneetkumarlamba@gmail.com)
© 2026 Published by Shahid Chamran University of Ahvaz

Abstract. Innovative computational biomechanics approaches are required to optimize the fractional dynamical behavior of non-small-cell lung cancer (NSCLC), which is one of the leading causes of cancer-related mortality on a global scale. This study presents a comprehensive fractional-order computational dynamical system describing the biomechanical interactions among tumor cells, cytotoxic $CD8^+$ T lymphocytes, and dendritic cells. The model is formulated as a set of nonlinear differential equations, and the memory effect and anomalous biological processes are introduced via the complex He transform. The equilibrium and stability analyses have provided critical values- for example, a basic reproduction number that governs the persistence or elimination of the tumor. The treatment model is a hybrid system, which entails continuous immune-tumor interactions and discrete therapeutic events. Computer modeling shows that, in cases of early surgical intervention followed by periodic chemotherapy, tumor burden decreases and the immune response is boosted. The results highlight the potential of mathematical modeling to enhance our comprehension of tumor–immune–therapy dynamics in NSCLC and to guide customized treatment planning.

Keywords: Non-small-cell Lung cancer, Fractional-order dynamics, Computational intervention dynamics and fractional control dynamics, Basic reproduction number.

1. Introduction

Lung cancer remains one of the greatest health problems in the world, as it causes millions of deaths every year and is the leading cause of cancer-related deaths [1]. Non-small-cell lung cancer (NSCLC), constituting almost 85 percent of lung cancers, is often diagnosed at late stages, leading to restricted treatment choices and poor survival rates [2]. Although targeted therapies and immunotherapies have improved the prognosis of late-stage patients with NSCLC, the current state of the disease is inconclusive, and new interventions that combine clinical interventions with a better comprehension of tumor-immune interactions are urgently needed. Mathematical modeling has become a potent method for overcoming this complication, as it provides predictive models to estimate disease evolution and necessary thresholds for tumor containment while testing therapeutic options [3]. Based on biological understanding and computational techniques, the quantitative framework of these models leads to optimized treatment schedules and individualized therapies. Specifically, more complex hybrid models, including continuous tumor-immune interactions and discrete clinical treatments involving computational control dynamics and biomechanical regulation, have shown effects in connecting theoretical analysis to real-world treatment regimens [4]. However, classical integer-order models are limited in their ability to capture hereditary and memory-dependent biological processes, such as immune exhaustion, tumor relapse, and delayed immune responses. Fractional calculus provides a promising alternative as it introduces memory effects into dynamical systems and thus offers a more realistic description of long-term tumor-immune interactions [5, 6]. Combining fractional-order dynamics with a hybrid therapeutic model is a new trend in mathematical oncology, which improves biological realism and clinical decision-making. Against this background, the subsequent subsections expound on the biological basis of tumor-immune interactions, the computational control dynamics, the biomechanical regulation, using the concept of fractional-order dynamics, and the objective and novelty of this study.

1.1. Tumor–immune system interactions

Lung cancer, especially NSCLC, is the most common subtype and a major cause of cancer-related deaths globally [1]. The immune system plays a paradoxical role in the development of cancer: on one hand, immune surveillance can destroy malignant cells, but on the other hand, tumors may adapt, become resistant to immune surveillance, and invigorate metastasis [7]. Cytotoxic

Published online: September 17 2026

$CD8^+$ T lymphocytes play a key role in this process by identifying tumor antigens presented by dendritic cells and triggering antigen-specific cytotoxicity [8]. However, this response is often compromised by tumor-induced immune suppression and exhaustion, and tumor persistence ensues. Mathematical models have been constructed to describe these dynamics, and it has been demonstrated that immune responses can result in tumor dormancy or destruction, depending on the parameter regimes [3]. These findings can be used to integrate immune dynamics into a therapeutic planning process.

1.2. Computational control dynamics and biomechanical regulation

Fractional-order computational regulation mechanisms play an important role in controlling nonlinear tumor–immune dynamical behavior in NSCLC systems. In early-stage cases, surgery is the main treatment, and chemotherapy is given in cycles to decrease the burden of the tumor and avoid future recurrences [2, 9]. Nonetheless, chemotherapy has a systemic effect, such as immunosuppression, which makes it difficult to combine with immune-based therapies.

To deal with nonlinear complexity, hybrid computational dynamical models are developed to integrate continuous tumor-immune biomechanics with discrete fractional-order control mechanisms [4]. Surgery is modeled as cytoreduction operations, and chemotherapy as a series of periodic perturbations of both malignant and immune cells. The hybrid method models treatment regimens, assesses long-term outcomes, and fills the gap between theory and practice.

1.3. Fractional-order dynamics and He's transform

Fractional-order computational modeling has recently gained considerable attention in biomechanics, computational oncology, and nonlinear dynamical systems because of its ability to capture hereditary effects, anomalous diffusion, and long-term memory-dependent biological responses. Several recent studies have demonstrated that fractional calculus provides more realistic representations of tumor progression, immune regulation, and biomechanical interactions compared with classical integer-order formulations. These developments further justify the adoption of fractional-order computational frameworks in modeling complex tumor–immune dynamical systems.

Although integer-order models have been useful in elucidating this phenomenon, they cannot capture hereditary and memory-dependent biological processes. Immune exhaustion, tumor relapse, and delayed immune reactions are inherently nonlocal phenomena that are more complex to describe with simple mathematical tools. Fractional calculus also introduces memory effects to dynamical systems, making it more realistic for cancer modeling [5, 6]. He's fractional complex transform reduces fractional differential equations to ordinary differential equations in the transformed time variable, retains hereditary effects, but allows for standard analysis [10]. In oncology, fractional-order-based models have shown the ability to model delayed immune responses and abnormal tumor behavior [4, 11].

Thus, fractional-order modeling provides a powerful extension to classical approaches, embedding biological memory into tumor–immune interactions. He et al. [12] examined how the morphology of gold nanoparticles influences blood flow in the vicinity of a wavy biological tissue wall and discussed its potential use in cancer treatment. Using gold nanoparticles in the slip cylinder, Wan Azmi et al. [13] established mathematical models of Casson fluid flow and described their implications in biomedicine. In the study by Almuneef et al., the bioheat equation under fractional derivatives was used to examine thermal damage in live tissue during thermotherapy [14]. Additionally, references [15-25] contain important work on fractional computational biomechanics modeling.

Recent advances in computational biomechanics and fractional dynamical system modeling have significantly improved the mathematical interpretation of tumor–immune interactions in complex biological systems. Contemporary studies have demonstrated that fractional-order computational frameworks provide more realistic representations of hereditary biological behavior, anomalous diffusion, delayed immune activation, and nonlinear tumor progression compared with classical integer-order formulations. In particular, modern techniques for biomechanical computation combined with nonlinear dynamical systems have been successfully applied to cancer progression, immune regulation, tissue interactions, and computational oncology dynamics.

Recent investigations published during 2024–2026 further emphasize the importance of fractional computational methods in describing multiscale biological interactions, memory-dependent dynamics, and long-term stability behavior in biomedical systems. These developments strongly motivate the present fractional-order computational biomechanics framework for non-small-cell lung cancer dynamics and enhance its relevance to JACM's scope.

1.4. Objectives and contributions

Based on these premises, the current research will attempt to establish a fractional-order hybrid mathematical model of NSCLC while incorporating tumor-immune interactions and discrete clinical interventions.

These contributions are particular and include:

- Formulate nonlinear fractional-order equations for tumor cells, $CD8^+$ T lymphocytes, and dendritic cells.
- Embed computational control dynamics and biomechanical regulation as discrete perturbations within continuous immune–tumor dynamics.
- Execute equilibrium, stability, and sensitivity analyses to find critical values like the basic reproduction number.
- Perform a numerical simulation to assess how timing, intensity, and frequency of treatment affect the effect of treatment under fractional dynamics.

These contributions together offer a theoretical basis for optimizing treatment regimens in NSCLC and insights into the interactions between tumor progression, immune dynamics, and therapeutic interventions.

1.5. Related work and novelty

Other mathematical models of NSCLC have mostly been based on integer-order ordinary differential equations [3, 4]. Although these models are informative for tumor-immune interactions and the most effective treatment regimens, they are weak in describing the effects of memory. Recent research has applied fractional calculus to cancer dynamics (including tumor stem cells) [11], combined virtual vitamin and chemotherapy regimens [13], and pollutant-induced skin cell injury [14].

This work is novel because it is the first to incorporate fractional calculus in a hybrid NSCLC treatment model that includes computational control dynamics and biomechanical regulation. The model predicts slower tumor decay, longer immune activation, and qualitatively different stability thresholds than classical models by embedding hereditary immune responses into discrete clinical interventions. This practice creates more biological realism and a basis for planning individual therapy. The current research follows this research question in two main aspects. We first adopt a framework of fractional-order dynamics formulated on He's complex transform, generalizing the classical ODE framework to capture hereditary and anomalous dynamics characteristic of cancer biology. The modeling of immune memory and delayed immune response, which cannot be represented in integer-order systems, is simplified with fractional calculus. We then build a hybrid treatment model that combines continuous tumor-immune interactions with discrete clinical therapies, including computational control dynamics and biomechanical regulation. This

composite model is closer to real-world treatment regimens, where immediate decreases in red blood cells and periodic therapy pulses on them play off with continuous immune surveillance. Equilibrium and stability studies, sensitivity analyses of the fractional-order parameters, and comparative studies all show that our model's results differ from those of integer-order methods. Specifically, faster tumor decay, longer immune response, and different stability thresholds are predicted by the impact of fractional dynamics, clarifying the significance of memory effects in treatment planning.

This paper will offer a new theoretical framework for optimizing NSCLC treatment approaches and build the biological realism of using fractional calculus by extending computational control dynamics and biomechanical regulation to a fractional-order immune-responsive system. Recent studies in computational biomechanics and fractional dynamical systems have demonstrated that memory-dependent formulations significantly improve the modeling accuracy of nonlinear biological systems. Modern computational oncology frameworks incorporate hereditary immune effects, delayed tumor responses, and multiscale biomechanical interactions through fractional-order dynamics. These recent developments motivate the present study and establish stronger connections between fractional computational mathematics and engineering-oriented biomechanical applications.

2. Metric of the Lung Cancer Fractional-Order Mathematical Model

The mathematical framework of the fractional-order lung cancer model is built from three coupled nonlinear differential equations that describe the dynamics of tumor cells, cytotoxic lymphocytes, and dendritic cells, as shown in Fig. 1. The system is expressed in fractional time using He's complex transform, which introduces hereditary and memory effects into the biological interactions:

$$\begin{aligned} \frac{\partial^\alpha T}{\partial T^\alpha} &= \alpha T(1-\beta T) - \gamma T - \phi CT \\ \frac{\partial^\alpha C}{\partial T^\alpha} &= vT - \eta CT - \kappa C \\ \frac{\partial^\alpha D}{\partial T^\alpha} &= \mu + \sigma DT - \rho CD - \omega D \end{aligned} \tag{1}$$

Assuming the fractional complex transform proposed by *He* and *Li*:

$$\xi = \frac{qt^\alpha}{\Gamma(1+\alpha)} \tag{2}$$

$$\frac{\partial^\alpha u}{\partial t^\alpha} = q\frac{\partial u}{\partial \xi}, \qquad u = T, C, D \tag{3}$$

Inverse of ξ, from Eq. (2):

$$t = \left(\frac{\Gamma(1+\alpha)}{q}\xi\right)^{\frac{1}{\alpha}} \tag{4}$$

This is consistent with the modified Riemann–Liouville framework, since the fractional derivative in physical time t is mapped into an ordinary derivative in the transformed variable ξ. As a result, the hereditary and memory-dependent effects of fractional dynamics are preserved while allowing the system to be analyzed with conventional ODE techniques. The governing equations in transformed time become:

$$\begin{aligned} \frac{\partial T}{\partial \xi} &= \frac{1}{q}[\alpha T(1-\beta T) - \gamma T - \phi CT] \\ \frac{\partial C}{\partial \xi} &= \frac{1}{q}[vT - \eta CT - \kappa C] \\ \frac{\partial D}{\partial \xi} &= \frac{1}{q}[\mu + \sigma DT - \rho CD - \omega D] \end{aligned} \tag{5}$$

Thus, the fractional complex transform effectively converts the nonlocal fractional-order system into a local ODE system in ξ, enabling rigorous analysis of positivity, boundedness, equilibrium, and stability while incorporating biological memory effects via fractional time scaling.

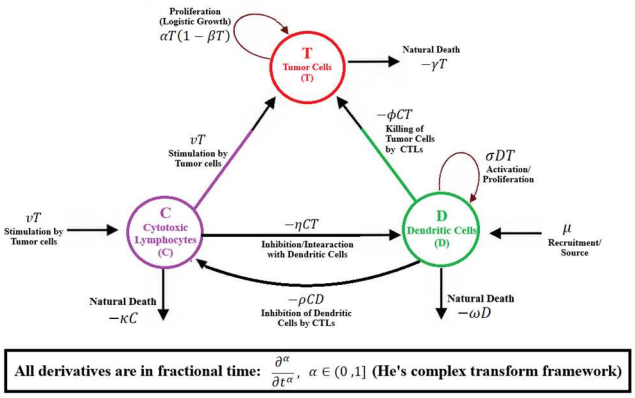

Fig. 1. Physical structure of fractional-order dynamics.

2.1. Determination of the fractional order parameter (α)

In this study, the fractional order parameter (α) is treated as a tunable parameter within the interval $(0 < \alpha \leq 1)$. By varying α, we capture different degrees of hereditary and memory effects in tumor-immune dynamics. Specifically, $\alpha = 1$ recovers the classical integer-order system, while values of $\alpha < 1$ introduce biologically realistic delays in immune activation, immune exhaustion, and slower tumor suppression. This qualitative exploration shows how fractional dynamics enrich the model's biological realism. Although the present work does not estimate α directly from empirical datasets, future research will focus on calibrating α using patient-specific data such as imaging-derived tumor volume trajectories, immune cell counts from biopsies, and survival outcomes from NSCLC clinical trials. Such calibration will enable quantitative validation and strengthen the framework's translational applicability for personalized treatment planning.

2.1.1. *Positivity*

Theorem 1: *If $T(0) > 0$ and $\gamma + \phi C > \alpha$, then $T(\xi) > 0$ for all $\xi > 0$.*
Proof: Fractional-order mathematical model of tumor cells is:

$$\frac{\partial T}{\partial \xi} = \frac{1}{q}[\alpha T(1 - \beta T) - \gamma T - \phi C T]$$
$$\frac{\partial T}{T[(\alpha - \gamma - \phi C) - \alpha\beta T]} = \frac{1}{q}\partial\xi \tag{6}$$

Using partial fraction decomposition:

$$\frac{\partial T}{T[(\alpha - \gamma - \phi C) - \alpha\beta T]} = \frac{1}{\alpha - \gamma - \phi C}\frac{1}{T} + \frac{\alpha\beta}{\alpha - \gamma - \phi C}\frac{1}{(\alpha - \gamma - \phi C) - \alpha\beta T} \tag{7}$$

$$\frac{1}{\alpha - \gamma - \phi C} ln\, T - \frac{1}{\alpha - \gamma - \phi C} ln[(\alpha - \gamma - \phi C) - \alpha\beta T] = \frac{\xi}{q} + C_1 \tag{8}$$

$$\frac{T}{(\alpha - \gamma - \phi C) - \alpha\beta T} = K e^{\frac{(\alpha - \gamma - \phi C)}{q}\xi} \tag{9}$$

where K depends on initial conditions and:

$$T(\xi) = \frac{(\alpha - \gamma - \phi C) K e^{\frac{(\alpha - \gamma - \phi C)}{q}\xi}}{1 + \alpha\beta K e^{\frac{(\alpha - \gamma - \phi C)}{q}\xi}} \tag{10}$$

Since the numerator and denominator are positive for $\gamma + \phi C > \alpha$, hence $T(\xi) > 0$. Now, replace ξ with t using the inverse transform and substitute, $\xi = (qt\hat{}\alpha)/\Gamma(1 + \alpha)$, we have:

$$T(t) = \frac{(\alpha - \gamma - \phi C) K e^{\left(\frac{(\alpha - \gamma - \phi C)}{\Gamma(1+\alpha)} t^{\alpha}\right)}}{1 + \alpha\beta K e^{\left(\frac{(\alpha - \gamma - \phi C)}{\Gamma(1+\alpha)} t^{\alpha}\right)}} \tag{11}$$

At $t = 0,\ T(0)$ fixes K,

$$K = \frac{T(0)}{(\alpha - \gamma - \phi C) - \alpha\beta T(0)} \tag{12}$$

$$T(t) = \frac{(\alpha - \gamma - \phi C)\frac{T(0)}{(\alpha - \gamma - \phi C) - \alpha\beta T(0)} e^{\left(\frac{(\alpha - \gamma - \phi C)}{\Gamma(1+\alpha)} t^{\alpha}\right)}}{1 + \alpha\beta\frac{T(0)}{(\alpha - \gamma - \phi C) - \alpha\beta T(0)} e^{\left(\frac{(\alpha - \gamma - \phi C)}{\Gamma(1+\alpha)} t^{\alpha}\right)}} \tag{13}$$

- When $\alpha = 1$, this reduces to the classical logistic solution in integer-order time.
- When $0 < \alpha < 1$, the growth/decay is governed by t^{α}, which reflects memory effects, i.e., tumor suppression is slower, consistent with fractional dynamics.

If $\gamma + \phi C > \alpha$, then positivity is proved.

Theorem 2: *If $C(0) > 0,\ \nu > 0$ and $\eta T + \kappa > 0$, then $C(\xi) > 0$ for all $\xi > 0$.*
Proof: Starting from:

$$\frac{\partial C}{\partial \xi} = \frac{1}{q}[\nu T - \eta C T - \kappa C] \tag{14}$$

We rewrite it as:

$$\frac{\partial C}{\partial \xi} + \frac{1}{q}(\eta T + \kappa) C = \frac{v}{q} T \tag{15}$$

This is a linear first-order ODE. The integrating factor is:

$$IF(\xi) = e^{\left(\frac{1}{q}\int(\eta T + \kappa)\xi\right)} \tag{16}$$

So, the solution becomes:

$$C(\xi) = \frac{1}{IF(\xi)}\left[C(0) + \frac{\nu}{q}\int_0^{\xi} T(s) IF(s) ds\right] \tag{17}$$

Since, $IF(\xi) > 0,\ C(0) > 0$ and the integrand is positive, we conclude $C(\xi) > 0$. This is an explicit solution in terms of the integrating factor and tumor trajectory $T(s)$.

Put $IF(\xi) > 0$ in $C(\xi)$:

$$C(\xi) = e^{\left(-\frac{1}{q}\int_0^{\xi}(\eta T(s)+\kappa)ds\right)}\left[C(0) + \frac{\nu}{q}\int_0^{\xi} T(s)e^{\left(\frac{1}{q}\int_0^{s}(\eta T(u)+\kappa)du\right)}ds\right] \tag{18}$$

Now, replacing ξ with the fractional time transform t using the inverse transform, substituting:

$$\xi = \frac{qt^{\alpha}}{\Gamma(1+\alpha)} \tag{19}$$

We obtain:

$$C(t) = e^{\left(-\frac{1}{q}\int_0^{\frac{qt^{\alpha}}{\Gamma(1+\alpha)}}(\eta T(s)+\kappa)ds\right)}\left[C(0) + \frac{\nu}{q}\int_0^{\frac{qt^{\alpha}}{\Gamma(1+\alpha)}} T(s)e^{\left(\frac{1}{q}\int_0^{s}(\eta T(u)+\kappa)du\right)}ds\right] \tag{20}$$

- When $\alpha = 1$, the transform reduces to the classical time, recovering the standard linear ODE solution.
- When $0 < \alpha < 1$, the upper limit of integration is fractional $((qt\hat{}\alpha)/\Gamma(1+\alpha))$, introducing memory effects into CD8⁺T dynamics.

This result shows that CD8⁺ T lymphocyte activation is hereditary under fractional dynamics. In practice, this models immune exhaustion and delayed responses; the immune system remembers past tumor states, so its cytotoxic activity is not instantaneous but distributed over time. This makes the fractional-order model more realistic than classical integer-order systems, especially for long-term tumor–immune interactions.

Theorem 3: *If $D(0) > 0,\ \mu > 0$ and $\sigma T > \rho C + \omega$, then $D(\xi) > 0$ for all $\xi > 0$.*

Proof: Starting from:

$$\frac{\partial D}{\partial \xi} = \frac{1}{q}[\mu + (\sigma T - \rho C - \omega)D] \tag{21}$$

We rewrite it as:

$$\frac{\partial D}{\partial \xi} - \frac{1}{q}(\sigma T - \rho C - \omega)D = \frac{\mu}{q} \tag{22}$$

This is a linear first-order ODE in $D(\xi)$. The integrating factor is:

$$IF(\xi) = e^{\left(-\frac{1}{q}\int(\sigma T - \rho C - \omega)\xi\right)} \tag{23}$$

So, the solution becomes:

$$D(\xi) = \frac{1}{IF(\xi)}\left[D(0) + \frac{\mu}{q}\int_0^{\xi} IF(s)ds\right] \tag{24}$$

Expanding explicitly:

$$D(\xi) = e^{\left(-\frac{1}{q}\int_0^{\xi}(\sigma T(s) - \rho C(s) - \omega)ds\right)}\left[D(0) + \frac{\mu}{q}\int_0^{\xi} e^{\left(-\frac{1}{q}\int_0^{s}(\sigma T(u) - \rho C(u) - \omega)du\right)}ds\right] \tag{25}$$

Now, replacing ξ with the fractional time transform $\xi = (qt\hat{}\alpha)/\Gamma(1+\alpha)$, we obtain:

$$D(t) = e^{\left(-\frac{1}{q}\int_0^{\frac{qt^{\alpha}}{\Gamma(1+\alpha)}}(\sigma T(s) - \rho C(s) - \omega)ds\right)}\left[D(0) + \frac{\mu}{q}\int_0^{\frac{qt^{\alpha}}{\Gamma(1+\alpha)}} e^{\left(-\frac{1}{q}\int_0^{s}(\sigma T(u) - \rho C(u) - \omega)du\right)}ds\right] \tag{26}$$

- When $\alpha = 1$, this reduces to the classical linear ODE solution.
- When $0 < \alpha < 1$, the fractional transform introduces memory effects, i.e., the upper limit of integration is fractional $((qt\hat{}\alpha)/\Gamma(1+\alpha))$, which means dendritic cells' dynamics depend on past tumor-immune interactions in a hereditary way.

As key antigen-presenting cells, dendritic cells evolve under fractional dynamics, remembering past tumor-immune interactions. Their activation or suppression accumulates over time, reflecting delayed immune priming and tolerance. With $IF(\xi) > 0,\ D(0) > 0$, and $\mu > 0$, the solution $D(\xi)$ remains positive, ensuring biological feasibility: dendritic cell populations stay bounded and meaningful even under fractional-order hereditary effects.

Theorem 4: *Positivity of Tumor, CD8⁺T, and Dendritic Cells in Fractional Time.*

Statement: Consider the fractional-order lung cancer model under He's complex transform with $0 < \alpha < 1$. For positive initial conditions $T(0) > 0,\ C(0) > 0,\ D(0) > 0$, the solutions $T(t),\ C(t),\ D(t)$ remain positive for all $t > 0$.

- When $\alpha = 1$, these solutions reduce to the classical integer-order ODE results.
- When $0 < \alpha < 1$, positivity is preserved; trajectories decay and grow slowly, consistent with biological hereditary effects.

Unlike integer-order models, where positivity is immediate, fractional positivity reflects hereditary effects- past states influence current dynamics, ensuring that tumor immune populations remain biologically meaningful, even with delayed responses.

2.1.1.1. *Boundedness*

Theorem 5: *For positive initial conditions, the total population $P(\xi) = T(\xi) + C(\xi) + D(\xi)$* remains bounded for all $\xi > 0$.

Proof: Differentiating the total population with respect to ξ:

$$\frac{dP}{d\xi} = \frac{dT}{d\xi} + \frac{dC}{d\xi} + \frac{dD}{d\xi} \tag{27}$$

Substituting the system equations:

$$\frac{dP}{d\xi} \leq \frac{1}{q}[\alpha T(1-\beta T) - \gamma T - \phi CT + \nu T - \eta CT - \kappa C + \mu + \sigma DT - \rho CD - \omega D] \tag{28}$$

Defining constant M as the maximum of coefficients such that $\frac{dP}{d\xi} \leq \frac{M}{q}P(\xi)$, and applying the fractional Gronwall inequality, we obtain:

$$P(\xi) \leq P(0)E_{\alpha}\left(\frac{M}{q}\xi^{\alpha}\right) \tag{29}$$

Since the Mittag-Leffler function E_{α} grows sub-exponentially, unlike the classical exponential function, the total population $P(\xi)$ remains bounded for all $\xi > 0$. This result ensures that the combined populations of tumor cells, CD8⁺ T lymphocytes, and dendritic cells do not diverge to infinity under fractional dynamics. Instead, they remain biologically feasible and bounded, reflecting realistic long-term tumor–immune interactions where growth is tempered by immune regulation and therapeutic interventions.

Theorem 6: *Tumor cells $T(\xi)$ remain bounded for all $\xi > 0$.*
Proof: The tumor dynamics satisfy:

$$\frac{\partial T}{\partial \xi} = \frac{1}{q}[(\alpha - \gamma - \phi C)T - \alpha\beta T^2] \tag{30}$$

This can be compared with the logistic equation:

$$\frac{\partial y}{\partial \xi} = \frac{1}{q}[(\alpha - \gamma - \phi C)y - \alpha\beta y^2] \tag{31}$$

where $y(\xi)$ approximates tumor growth.
Defining:

$$r = \frac{(\alpha - \gamma - \phi C)}{q}\ , \quad K = \frac{(\alpha - \gamma - \phi C)}{\alpha\beta} \tag{32}$$

where r is the effective growth rate and K is the carrying capacity. The logistic solution is:

$$y(\xi) = \frac{K}{1 + \left(\frac{K - y_0}{y_0}\right)e^{-r\xi}} \tag{33}$$

where $y_0 = y(0)$. Substituting Eq. (32), we get:

$$y(\xi) = \frac{\frac{(\alpha - \gamma - \phi C)}{\alpha\beta}}{1 + \left(\frac{\frac{\alpha - \gamma - \phi C}{\alpha\beta} - y_0}{y_0}\right)e^{\left(-\frac{\alpha - \gamma - \phi C}{q}\xi\right)}} \tag{34}$$

Since $T(\xi) \leq y(\xi)$, tumor cells are bounded above by the logistic solution. Using the fractional transform $\xi = (qt\hat{}\alpha)/\Gamma(1+\alpha)$:

$$y(t) = \frac{\frac{(\alpha - \gamma - \phi C)}{\alpha\beta}}{1 + \left(\frac{\frac{\alpha - \gamma - \phi C}{\alpha\beta} - y_0}{y_0}\right)e^{\left(-\frac{\alpha - \gamma - \phi C}{\Gamma(1+\alpha)}t^{\alpha}\right)}} \tag{35}$$

For $\alpha = 1$ (integer-order), this reduces to the classical logistic solution.
For $0 < \alpha < 1$ (fractional-order), the exponential decay term depends on t^{α}, producing slower convergence and modeling memory effects.
Fractional boundedness means the system takes longer to settle at its maximum level. This shows that tumor cells may linger before being controlled, sometimes returning, because the immune system remembers the past and reacts more slowly.

Theorem 7: *CD8⁺T cells $C(\xi)$ remain bounded for all $\xi > 0$.*
Proof: The CD8⁺T cell dynamics satisfy:

$$\frac{\partial C}{\partial \xi} + \frac{1}{q}(\eta T + \kappa)C = \frac{v}{q}T \tag{36}$$

This is a linear first-order ODE. The integrating factor is:

$$IF(\xi) = e^{\left(\frac{1}{q}\int(\eta T + \kappa)\xi\right)} \tag{37}$$

Hence, the explicit solution is:

$$IF(\xi) = e^{\left(\frac{1}{q}\int(\eta T + \kappa)\xi\right)}C(\xi) = \frac{1}{IF(\xi)}\left[C(0) + \frac{\nu}{q}\int_0^{\xi} T(s)IF(s)ds\right] \tag{38}$$

Since, $T(S)$ is bounded and $IF(\xi)$ grows exponentially, the integral remains finite. Thus $C(\xi)$ is bounded. Expanding explicitly:

$$C(\xi) = e^{\left(-\frac{1}{q}\int_0^{\xi}(\eta T(s)+\kappa)ds\right)}\left[C(0) + \frac{\nu}{q}\int_0^{\xi} T(s)e^{\left(\frac{1}{q}\int_0^{s}(\eta T(u)+\kappa)du\right)}ds\right] \tag{39}$$

Using the fractional complex transform $\xi = (qt\hat{}\alpha)/\Gamma(1+\alpha)$:

$$C(t) = e^{\left(-\frac{1}{q}\int_0^{\frac{qt^{\alpha}}{\Gamma(1+\alpha)}}(\eta T(s)+\kappa)ds\right)}\left[C(0) + \frac{\nu}{q}\int_0^{\frac{qt^{\alpha}}{\Gamma(1+\alpha)}} T(s)e^{\left(\frac{1}{q}\int_0^{s}(\eta T(u)+\kappa)du\right)}ds\right] \tag{40}$$

- For $\alpha = 1$, this reduces to the classical bounded linear ODE solution.
- For $0 < \alpha < 1$, the fractional transform introduces memory effects; CD8⁺ T cell dynamics depend on past tumor-immune interactions.

Thus, $C(\xi)$ remain bounded for all $\xi > 0$.

Theorem 8: *Dendritic cells $T(\xi)$ remain bounded for all $\xi > 0$.*
Proof: The dendritic cell dynamics satisfy:

$$\frac{\partial D}{\partial \xi} - \frac{1}{q}(\sigma T - \rho C - \omega)D = \frac{\mu}{q} \tag{41}$$

This is a linear first-order ODE. The integrating factor is $IF(\xi) = e\hat{}((-1/q\int(\sigma T - \rho C - \omega)\xi))$. Hence, the explicit solution is:

$$D(\xi) = \frac{1}{IF(\xi)}\left[D(0) + \frac{\mu}{q}\int_0^{\xi} IF(s)ds\right] \tag{42}$$

Since, $IF(\xi) > 0$ and the integral is finite (because $T(\xi)$, $C(\xi)$ are bounded), therefore $D(\xi)$ is bounded, so:

$$D(\xi) = e^{\left(-\frac{1}{q}\int_0^{\xi}(\sigma T(s)-\rho C(s)-\omega)ds\right)}\left[D(0) + \frac{\mu}{q}\int_0^{\xi} e^{\left(-\frac{1}{q}\int_0^{s}(\sigma T(u)-\rho C(u)-\omega)du\right)}ds\right] \tag{43}$$

Using the fractional complex transform $\xi = (qt\hat{}\alpha)/\Gamma(1+\alpha)$, we have:

$$D(t) = e^{\left(-\frac{1}{q}\int_0^{\frac{qt^{\alpha}}{\Gamma(1+\alpha)}}(\sigma T(s)-\rho C(s)-\omega)ds\right)}\left[D(0) + \frac{\mu}{q}\int_0^{\frac{qt^{\alpha}}{\Gamma(1+\alpha)}} e^{\left(-\frac{1}{q}\int_0^{s}(\sigma T(u)-\rho C(u)-\omega)du\right)}ds\right] \tag{44}$$

This boundedness ensures that dendritic cells, which are essential for antigen presentation and immune activation, remain biologically feasible under fractional dynamics. Their population does not diverge but instead reflects hereditary immune behavior, where activation or suppression depends on accumulated past tumor–immune interactions. This model delays immune priming and tolerance, adding realism to tumor–immune system modeling.

3. Existence and Uniqueness of the Solution

Lemma 9: *The vector field $F(T, C, D) = (f, g, h)$ is C^1 on R^3. Hence, for any initial condition $(T_0, C_0, D_0) \in R^3$, there exists a unique local solution $(T(\xi), C(\xi), D(\xi))$ on some interval $[0, \xi_{max}$. Moreover, the solution depends continuously on the initial data.*
Proof: Let $q \neq 0$ and all parameters $\alpha, \beta, \gamma, \phi, \nu, \eta, \kappa, \mu, \sigma, \rho, \omega$ be finite constants.
Consider the IVP, $\frac{d}{d\xi}\begin{bmatrix}T\\C\\D\end{bmatrix} = \begin{bmatrix}f(T,C,D)\\g(T,C,D)\\h(T,C,D)\end{bmatrix}$, $\begin{bmatrix}T(0)\\C(0)\\D(0)\end{bmatrix} = \begin{bmatrix}T_0\\C_0\\D_0\end{bmatrix}$ with:

$$f(T, C, D) = \frac{dT}{d\xi} = \frac{1}{q}[\alpha T(1 - \beta T) - \gamma T - \phi CT] \tag{45}$$

$$g(T, C, D) = \frac{dC}{d\xi} = \frac{1}{q}[\upsilon T - \eta CT - \kappa C] \tag{46}$$

$$h(T, C, D) = \frac{dD}{d\xi} = \frac{1}{q}[\mu + \sigma DT - \rho CD - \omega D] \tag{47}$$

Partial derivatives of f, g, h with respect to T, C, D are:

$$\frac{\partial f}{\partial T} = \frac{1}{q}[-\gamma - \phi C - \alpha(\beta T - 1) - \alpha\beta T] \quad \Rightarrow \left|\frac{\partial f}{\partial T}\right| = \frac{1}{q}[\alpha(1 - 2\beta T) - \gamma - \phi C] \leq \frac{M}{\mu_1} < \infty \tag{48}$$

$$\frac{\partial f}{\partial C} = \frac{1}{q}[-\phi T] \quad \Rightarrow \left|\frac{\partial f}{\partial T}\right| = \frac{\phi T}{q} \leq \frac{M}{\mu_1} < \infty \tag{49}$$

$$\frac{\partial f}{\partial D} = 0 \quad \Rightarrow \left|\frac{\partial f}{\partial D}\right| = 0 \leq \frac{M}{\mu_1} < \infty \tag{50}$$

$$\frac{\partial g}{\partial T} = \frac{1}{q}[\nu - \eta C] \quad \Rightarrow \left|\frac{\partial g}{\partial T}\right| = \frac{-\nu + \eta C}{q} \leq \frac{M}{\mu_1} < \infty \tag{51}$$

$$\frac{\partial g}{\partial C} = \frac{1}{q}[-\eta T - \kappa] \quad \Rightarrow \left|\frac{\partial g}{\partial C}\right| = \frac{\kappa + \eta T}{q} \leq \frac{M}{\mu_1} < \infty \tag{52}$$

$$\frac{\partial g}{\partial D}=0 \quad \Rightarrow \left|\frac{\partial g}{\partial D}\right|=0\leq\frac{M}{\mu_1}<\infty \tag{53}$$

$$\frac{\partial h}{\partial T}=\frac{1}{q}[\sigma D] \quad \Rightarrow \left|\frac{\partial h}{\partial T}\right|=\frac{\sigma D}{q}\leq\frac{M}{\mu_1}<\infty \tag{54}$$

$$\frac{\partial h}{\partial C}=\frac{1}{q}[-\rho D] \quad \Rightarrow \left|\frac{\partial h}{\partial C}\right|=\frac{\rho D}{q}\leq\frac{M}{\mu_1}<\infty \tag{55}$$

$$\frac{\partial h}{\partial D}=\frac{1}{q}[\sigma T-\rho C-\omega] \quad \Rightarrow \left|\frac{\partial h}{\partial D}\right|=\frac{1}{q}[-\sigma T+\rho C+\omega]\leq\frac{M}{\mu_1}<\infty \tag{56}$$

Each component of F is a polynomial (quadratic) in (T,C,D), scaled by $\frac{1}{q}$ polynomials are C^{∞}, so $F\in C^1(R^3)$. A C^1 vector field is locally *Lipschitz* on R^3. By the *Picard-Lindelof* theorem, the IVP admits a unique local solution through any initial point, with continuous dependence on initial data. The solution can be continued as long as it remains bounded; thus, a unique maximal solution exists.

4. Equilibrium Analysis

The system of equilibrium equations is:

$$\alpha T(1-\beta T)-\gamma T-\phi CT=0 \tag{57}$$

$$\upsilon T-\eta CT-\kappa C=0 \tag{58}$$

$$\mu+\sigma DT-\rho CD-\omega D=0 \tag{59}$$

Case 1: *Tumor-free equilibrium* $(T=0)$:
With initial conditions $T=0$, $C=0$, $D=\mu/\omega$, the equilibrium point is:

$$E_0=(T,C,D)=\left(0,0,\frac{\mu}{\omega}\right) \tag{60}$$

This corresponds to complete tumor eradication, with the immune system at baseline dendritic cell.
Case 2: *Coexistence equilibrium* $(T>0,\ C>0,\ D>0)$:

$$\nu T-\eta CT-\kappa C=0 \quad \Rightarrow \quad C=\frac{\nu T}{\eta T+\kappa} \tag{61}$$

Substituting into the tumor equation, we get:

$$T(\alpha-\gamma-\alpha\beta T-\phi C)=0 \tag{62}$$

$$T>0, \qquad \alpha-\gamma-\alpha\beta T-\phi C=0 \quad \Rightarrow \quad \phi C=\alpha-\gamma-\alpha\beta T \tag{63}$$

Replacing $C=\nu T/(\eta T+\kappa)$, we get:

$$\alpha\beta\eta T^2+(\phi\nu+\alpha\beta\kappa-(\alpha-\gamma)\eta)T-(\alpha-\gamma)\kappa=0 \tag{64}$$

The quadratic can be written as:

$$AT^2+BT+C=0 \tag{65}$$

where,

$$A=\alpha\beta\eta, \quad B=\phi\nu+\alpha\beta\kappa-(\alpha-\gamma)\eta, \quad C=-(\alpha-\gamma)\kappa \tag{66}$$

The roots are:

$$T^*=\frac{-B\pm\sqrt{\Delta}}{2A},\ \Delta=(\phi\nu+\alpha\beta\kappa-(\alpha-\gamma)\eta)^2+4\alpha\beta\eta(\alpha-\gamma)\kappa \tag{67}$$

Corresponding equilibrium values are $\hat{C}^*=(\nu\hat{T}^*)/(\eta\hat{T}^*+\kappa),\ \hat{D}^*=\mu/(\rho\hat{C}^*+\omega-\sigma\hat{T}^*)$.
Feasibility requires $\rho C^*+\omega-\sigma T^*>0 \quad \Rightarrow \quad D^*>0$. Thus, the coexistence equilibrium is:

$$E^*=\left(T^*,\ \frac{\nu T^*}{\eta C+\kappa},\ \frac{\mu}{\rho C^*+\omega-\sigma T^*}\right) \tag{68}$$

In equilibrium analysis, two outcomes are possible. The tumor-free equilibrium E_0 represents complete eradication, with dendritic cells at baseline and stability achieved when immune strength exceeds tumor growth $(\gamma>\alpha)$. The coexistence equilibrium (E^*) occurs when tumor cells, $CD8^+$ T lymphocytes, and dendritic cells all persist at positive levels. Here, the tumor is not eliminated but remains regulated by immune activity, provided $\rho C^*+\omega>\sigma T^*$. Biologically, E_0 reflects successful clearance, while E^* models controlled persistence or dormancy under immune surveillance.

5. Basic Reproduction Number

The tumor dynamics are given by:

$$\frac{\partial T}{\partial\xi}=\frac{1}{q}[\alpha T-\alpha\beta T^2-\gamma T-\phi CT] \tag{69}$$

Let (T^*, C^*, D^*) be an equilibrium. Define $x = T - T^*$, keeping $C \approx C$. Linearizing RHS in x gives:

$$\frac{\partial x}{\partial \xi} = \frac{1}{q}(\alpha x - (2\alpha\beta T^* + \gamma + \phi C^*)x) \tag{70}$$

- Gain (new tumor production): $F = \alpha/q$.
- Loss (removal): $V = (2\alpha\beta\hat{T}^* + \gamma + \phi\hat{C}^*)/q$.

The next-generation number is:

$$R_0 = \frac{F}{V} = \frac{\alpha}{2\alpha\beta T^* + \gamma + \phi C^*} \tag{71}$$

Tumor-free equilibrium, at $E_0 = (0,0,\frac{\mu}{\omega})$, we get $T^* = 0\ ,\ C^* = 0$ then:

$$F = \frac{\alpha}{q}, \quad V = \frac{\gamma}{q}, \quad R_0 = \frac{\alpha}{\gamma} \tag{72}$$

- If $R_0 < 1$; Tumor cells decay exponentially, and the tumor-free equilibrium is stable.
- If $R_0 > 1$; Tumor cells grow, and the tumor persists.

5.1. Biological interpretation of R_0

In the tripartite tumor–immune system, the basic reproduction number R_0 represents the expected number of new tumor cells generated from a single tumor cell in the presence of immune surveillance. Biologically, the numerator (α) reflects the intrinsic proliferative capacity of tumor cells, while the denominator $(2\alpha\beta T^* + \gamma + \phi C^*)$ captures the combined suppressive effects of tumor self-limitation, cytotoxic CD8⁺ T lymphocyte activity, and dendritic cell–mediated immune regulation. Thus, R_0 quantifies the balance between tumor growth and immune removal.

- If $R_0 < 1$, immune mechanisms dominate: CD8⁺ T cells and dendritic cells eliminate tumor cells faster than they can proliferate, leading to tumor eradication.
- If $R_0 > 1$, tumor proliferation exceeds immune suppression, resulting in persistence or progression of disease.

In this framework, R_0 serves as a threshold parameter linking mathematical stability analysis to biological outcomes. It provides a predictive criterion for whether the system stabilizes at the tumor-free equilibrium or at coexistence equilibrium, where tumor cells persist under immune surveillance. This interpretation underscores the clinical relevance of R_0 as a biomarker for treatment efficacy and immune competence in NSCLC.

6. Analysis of the System's Stability at the Equilibrium

For the tumor dynamics:

$$F_T(T, C, D) = \alpha T - \alpha\beta T^2 - \gamma T - \phi CT \tag{73}$$

$$\frac{\partial F_T}{\partial T} = \alpha(1 - 2\beta T) - \gamma - \phi C, \quad \frac{\partial F_T}{\partial C} = -\phi C, \quad \frac{\partial F_T}{\partial D} = 0 \tag{74}$$

For CD8⁺T cells:

$$F_C(T, C, D) = \nu T - \eta CT - \kappa C \tag{75}$$

$$\frac{\partial F_C}{\partial T} = \nu - \eta C, \quad \frac{\partial F_C}{\partial C} = -(\eta T - \kappa), \quad \frac{\partial F_C}{\partial D} = 0 \tag{76}$$

For dendritic cells:

$$F_D(T, C, D) = \mu + \sigma DT - \rho CD - \omega D \tag{77}$$

$$\frac{\partial F_D}{\partial T} = \sigma D, \quad \frac{\partial F_C}{\partial C} = -\rho D, \quad \frac{\partial F_C}{\partial D} = \sigma T - \rho C - \omega \tag{78}$$

The Jacobian matrix is:

$$J(T, C, D) = \begin{bmatrix} \alpha(1 - 2\beta T) - \gamma - \phi C & -\phi C & 0 \\ \nu - \eta C & -(\eta T - \kappa) & 0 \\ \sigma D & -\rho D & \sigma T - \rho C - \omega \end{bmatrix} \tag{79}$$

The fractional system Jacobian is J/q. Jacobian at tumor-free equilibrium $E_0 = (0,0,\frac{\mu}{\omega})$ is:

$$J(E_0) = \begin{bmatrix} \alpha - \gamma & 0 & 0 \\ \nu & -\kappa & 0 \\ 0 & -\rho\frac{\mu}{\omega} & -\omega \end{bmatrix} \tag{80}$$

Eigenvalues are:

$$\lambda_T = \frac{\alpha - \gamma}{q}, \quad \lambda_C = \frac{-\kappa}{q} < 0, \quad \lambda_D = \frac{-\omega}{q} < 0 \tag{81}$$

Stability of E_0;

- If $\gamma > \alpha$, then $\lambda_T < 0$ and all eigenvalues are negative, so E_0 is locally asymptotically stable.
- If $\gamma < \alpha$, then $\lambda_T > 0$, making E_0 unstable.

Theorem 10: If $\gamma > \alpha \ \left(\approx R_0 = \frac{\alpha}{\gamma} < 1\right)$, then $\lambda_T < 0$ and all eigenvalues are negative; E_0 is locally asymptotically stable. If $\gamma < \alpha$, then $\lambda_T > 0$ and E_0 is unstable.

Proof: Let the endemic equilibrium $E_1 = (T^*, C^*, D^*)$ satisfy:

$$\alpha T^*(1 - \beta T^*) - \gamma T^* - \phi C^* T^* = 0 \tag{82}$$

$$vT^* - (\eta T^* + \kappa)C^* = 0 \tag{83}$$

$$\mu + (\sigma T^* - \rho C^* - \omega)D^* = 0 \tag{84}$$

Assume $T^* > 0, \quad C^* > 0, \quad D^* > 0$. Jacobian at (E_1) ; substitute (T^*, C^*, D^*):

$$J(E_1) = \begin{bmatrix} \alpha(1 - 2\beta T^*) - \gamma - \phi C^* & -\phi T^* & 0 \\ v - \eta C^* & -(\eta T^* + \kappa) & 0 \\ \sigma D^* & -\rho D^* & (\sigma T^* - \rho C^* - \omega) \end{bmatrix} \tag{85}$$

Lemma 11: *The eigenvalue associated with dendritic cells is* $\lambda_D = (\sigma \hat{T}^* - \rho \hat{C}^* - \omega)/q$. *Hence* $\lambda_D < 0$ *if* $\omega + \rho C^* > \sigma T^*$.

Define:

$$A = \begin{bmatrix} \alpha(1 - 2\beta T^*) - \gamma - \phi C^* & -\phi T^* \\ v - \eta C^* & -(\eta T^* + \kappa) \end{bmatrix} \tag{86}$$

$$tr(A) = \alpha(1 - 2\beta T^*) - \gamma - \phi C^* - (\eta T^* + \kappa) \tag{87}$$

$$det(\, A) = -[\alpha(1 - 2\beta T^*) - \gamma - \phi C^*](\eta T^* + \kappa) - \phi T^*(v - \eta C^*) \tag{88}$$

Since, ξ-Jacobian is A/q, the eigenvalues are roots of $(P(\lambda))/q$.

Lemma 12: *The two eigenvalues of the tumor-* CD8⁺T *cells have negative real parts if* $tr(A) < 0$ *and* $det(\, A) > 0$.

Proof: Routh-Hurwitz criteria, using the equilibrium relation, it is often useful to express $(v - \eta C^*)$ CD8⁺T equilibrium put in $\det(A)$,

$$\det(A) = -[\alpha(1 - 2\beta T^*) - \gamma - \phi C^*](\eta T^* + \kappa) - \phi \kappa C^* \tag{89}$$

Similarly, tumor equilibrium:

$$\alpha(1 - 2\beta T^*) - \gamma - \phi C^* = -\alpha \beta T^* \tag{90}$$

$tr(A) = -\alpha\beta T^* - (\eta T^* + \kappa) < 0$ strictly negative for $T^* > 0$,

$$det(\, A) = \alpha \beta T^*(\eta T^* + \kappa) + \phi \kappa C^* > 0 \tag{91}$$

$\therefore$ The tumor-CD8⁺T cells are automatically stable at (E_1) a given $T^* > 0, C^* > 0$ and positive parameter.

Theorem 13: Local Stability of $\boldsymbol{E_1}$

Suppose $T^* > 0, C^* > 0, D^* > 0$ *satisfies the equilibrium equation; then Tumor-*CD8⁺T *is always stable, because* $tr(A) = -\alpha\beta T^* - (\eta T^* + \kappa) < 0$ *and* $det(\, A) = \alpha\beta T^*(\eta T^* + \kappa) + \phi\kappa C^* > 0$. E_1 *is locally asymptotically stable iff the dendritic eigenvalue is negative:* $\lambda_D = \frac{\sigma T^* - \rho C^* - \omega}{q} < 0 \quad \Leftrightarrow \quad \omega + \rho C^* > \sigma T^*$.

Proof: At E_1, the tumor reproduction ratio (i.e., next generation) is $R_0 = \alpha/(2\alpha\beta\hat{T}^0 + \gamma + \phi\hat{C}^*)$

Using the tumor equilibrium identity $\alpha(1 - \beta T^*) - \gamma - \phi C^* = 0$, we get:

$$2\alpha\beta T^* + \gamma + \phi C^* = \alpha\beta T^* + \alpha \tag{92}$$

$$R_0 = \frac{1}{\beta T^* + 1} < 1 \tag{93}$$

Thus, $R_0 < 1$ automatically at E_1, consistent with the negative trace result. Stability hinges solely on dendritic direction $\omega + \rho C^* > \sigma T^*$.

6.1. Characteristics of states for equilibrium values with respect to α

At equilibrium, the system satisfies:

$$vT^* - \eta C^* T^* - \kappa C^* = 0 \tag{94}$$

$$\mu + \sigma D^* T^* - \rho C^* D^* - \omega D^* = 0 \tag{95}$$

$$f(T^*, C^*, \alpha) = T^*(\alpha(1 - \beta T^*) - \gamma T^* - \phi C^* T^*) = 0 \tag{96}$$

From them:

$$\begin{gathered} g(T^*, C^*) = vT^* - (\eta T^* + \kappa)C^* = 0 \\ C^* = \frac{vT^*}{\eta T^* + \kappa} \\ h(T^*, C^*, D^*) = \mu + (\sigma T^* - \rho C^* - \omega)D^* = 0 \end{gathered} \tag{97}$$

$$D^* = \frac{\mu}{\rho C^* + \omega - \sigma T^*} \tag{98}$$

6.2. Sensitivity of tumor equilibrium to α

Differentiating the tumor equilibrium condition gives:

$$\frac{dT^*}{d\alpha} = -\frac{T^*(1-\beta T^*)}{\alpha(1-2\beta T^*) - \gamma - \phi C^* - \frac{\phi T^*(v-\eta C^*)}{\eta T^* + \kappa}} \tag{99}$$

This expression shows the implicit sensitivity of tumor equilibrium to changes in α. If α increases, the sign of the denominator determines whether T^* grows or declines.

6.3. Sensitivity of CD8⁺T cells to α

$$\frac{dC^*}{d\alpha} = \frac{v\kappa}{(\eta T^* + \kappa)^2}\frac{dT^*}{d\alpha} \tag{100}$$

Thus, CD8⁺ T cell equilibrium depends directly on the tumor equilibrium's sensitivity to α.

$$\frac{dD^*}{d\alpha} = \frac{-\mu\left(\frac{\rho v\kappa}{(\eta T^* + \kappa)^2} - \sigma\right)\frac{dT^*}{d\alpha}}{(\rho C^* + \omega - \sigma T^*)^2} \tag{101}$$

Hence, dendritic cell equilibrium shifts according to both tumor and CD8⁺T cell responses to α.

7. Nature of Tumor Cells when CD8⁺T Cells Are Nondecreasing

The tumor dynamics satisfy:

$$\frac{\partial T}{\partial t} = T(\alpha - \alpha\beta T) - \gamma - \phi C(t)) \tag{102}$$

Define the time-varying net growth rate $A(t) = \alpha - \gamma - \phi C(t)$, so that $dT/dt = (A(t) - \alpha\beta T)$.
If $C(t)$ is nondecreasing, then $A(t)$ is nonincreasing because $-\phi C(t)$ becomes more negative or stays the same. Hence, $t \geq 0$.

$$\therefore \quad A(t) \leq A(0) = \alpha - \gamma - \phi C(0) \tag{103}$$

7.1. Comparison with Logistic equation

Consider the logistic comparison equation:

$$\frac{dy}{dt} = y(A(0) - \alpha\beta y), \quad y(0) = T(0) \tag{104}$$

Since $A(t) \leq A(0)$, we have:

$$\frac{dT}{dt} = T(A(t) - \alpha\beta T) \leq T(A(0) - \alpha\beta T) \tag{105}$$

By the comparison principle for ODEs, i.e., with the same initial conditions, since the RHS of T is bounded above by that of y, it follows that $T(t) \leq y(t)\ \forall\ t \geq 0$.
The explicit solution of the logistic comparison equation is:

$$y(t) = \frac{A_0 y_0}{\alpha\beta y_0 + (A_0 - \alpha\beta y_0)e^{-A_0 t}}\ , \quad y_0 = T(0) \tag{106}$$

- If $A_0 > 0$ then $\lim_{t\to\infty} y(t) = \frac{A_0}{\alpha\beta}$.
- If $A_0 < 0$ then $y(t)$ is nonincreasing & tending to 0 as $t \to \infty$.

Thus,

$$y(t) \leq max\left\{y_0, \frac{A_0}{\alpha\beta}\right\} \tag{107}$$

By comparison, $T(t) \leq y(t)$:

$$\therefore \quad T(t) \leq max\left\{T(0), \frac{\alpha - \gamma - \phi C(0)}{\alpha\beta}\right\} \quad \forall\ t \geq 0 \tag{108}$$

If:

$$T(0) > \frac{\alpha - \gamma - \phi C(0)}{\alpha\beta} \quad \Rightarrow\ \alpha(1 - \beta T(0)) - \gamma - \phi C(0) \leq 0 \tag{109}$$

then $y(t)$ is nonincreasing, and the equality preserves monotonicity: $T(t) \leq T(0) \quad \forall\ t \geq 0$.

- The tumor never exceeds its initial value if the initial immune pressure is strong enough or the initial tumor load is large enough to make the net growth term nonpositive at $t = 0$. If $T(0) < (\alpha - \gamma - \phi C(0))/\alpha\beta$, then the tumor can initially grow. However, because $A(t)$is nonincreasing, the effective carrying level diminishes over time, and the bound still holds: $T(t) \leq (\alpha - \gamma - \phi C(0))/\alpha\beta \quad \forall\ t \geq 0$

- A common nondecreasing form is a saturating response known as the nondecreasing CD8⁺T trajectory, i.e. $C(t) = (C_1 t)/(1 + C_2 t)$ then $A(t) = \alpha - \gamma - \phi_1 (C_1 t)/(1 + C_2 t)$ is strictly decreasing and approaches $\alpha - \gamma - \phi_1 C_1 / C_2$. The same bounds apply, and if the initial cap condition holds, the tumor never exceed $T(0)$.
- When CD8⁺T cells are nondecreasing, the tumor population is uniformly bounded by:

$$T(t) \leq max \left\{ T(0), \frac{\alpha - \gamma - \phi C(0)}{\alpha \beta} \right\}, \quad \forall\ t \geq 0 \tag{110}$$

ensuring that immune pressure prevents unbounded tumor growth and, under strong initial conditions, the tumor never exceeds its starting level.

- If $T(t) \geq (\alpha - \gamma - \phi C(0))/\alpha\beta$, then $T(t) \leq T(0) \quad \forall\ t \geq 0$, the tumor never exceeds its initial value.

8. Tumor Cell Convergence when CD8⁺T Cells Remain Constant

The tumor converges to zero when the net growth rate is negative. With $C(t) \equiv C_0$, the tumor dynamics reduce to $\partial T/\partial t = T(\alpha(1 - \beta T) - \gamma - \phi C_0) = T(A_0 - \alpha\beta T)$ where $A_0 = \alpha - \gamma - \phi C_0$. This is a logistic-type ODE with a linear growth rate A_0 and saturation coefficient $\alpha\beta > 0$,

$$\frac{dT}{T(A_0 - \alpha\beta T)} = dt \tag{110}$$

$$\frac{1}{T(A_0 - \alpha\beta T)} = \frac{1}{A_0}\frac{1}{T} + \frac{\alpha\beta}{A_0}\frac{1}{A_0 - \alpha\beta T} \tag{111}$$

$$ln \left| \frac{T}{A_0 - \alpha\beta T} \right| = A_0 t + C, \frac{T}{A_0 - \alpha\beta T} = K e^{A_0 t} \tag{112}$$

where,

$$T(t) = \frac{A_0 K e^{A_0 t}}{1 + \alpha\beta K e^{A_0 t}} \tag{113}$$

Using:

$$T(0) = T_0, T_0 = \frac{A_0 K}{1 + \alpha\beta K}, K = \frac{T_0}{A_0 - \alpha\beta T_0}, y(t) = \frac{A_0 T_0}{\alpha\beta T_0 + (A_0 - \alpha\beta T_0) e^{-A_0 t}} \tag{114}$$

Conditions for convergence:

- If $A_0 < 0$ (net growth is negative) then $\lim_{t\to\infty} e^{A_0 t} = 0 \quad \Rightarrow \quad \lim_{t\to\infty} T(t) = 0$ i.e., the tumor converges to zero.
- If $A_0 = 0$; the ODE becomes $dT/dt = -\alpha\beta \hat{T}^2$ and $T(t) = \frac{T_0}{1 + \alpha\beta T_0 t} \to 0$ as $t \to \infty$.
- If $A_0 > 0$, net growth is positive, then $\lim_{t\to\infty} T(t) = \frac{A_0}{\alpha\beta} > 0$, the positive equilibrium.
- $\alpha - \gamma - \phi C_0 \leq 0$, i.e., the combined killing by dendritic cells and CD8⁺T cells outweighs intrinsic tumor growth.

9. Results

9.1. Numerical simulation

To investigate the impact of fractional-order dynamics on tumor–immune interactions, numerical simulations were performed for $\alpha = 0.25, 0.5, 0.75, 1$ over a period of 350 days. The trajectories of tumor cells, CD8⁺ T lymphocytes, and dendritic cells were analyzed to assess how memory effects influence system behavior.

- **Tumor cells (blue, dashed):** At lower fractional orders $(\alpha = 0.25, 0.5)$, tumor growth decelerates, and the peak increases longer before it is suppressed. At $\alpha = 1$, which is the classical integer order, tumor decay is stiffer and more abrupt. This indicates that the tumor's survival depends on hereditary components, extended by the use of fractional dynamics.
- **CD8⁺ T cells (red, solid):** These are the immune cells, which reach their peak after tumor growth, at around day 150.

Smaller αleads to weaker but longer-lasting activation of CD8⁺ and indicates immune exhaustion and slower surveillance. When $\alpha = 1$, the immune response is more concentrated and stronger, as expected of standard ODE behavior.

- **Dendritic cells (orange, dotted):** Dendritic cell activation is less stochastic and more general, peaking at around 15 days.

Dendritic dynamics are more diffuse at lower fractional orders, indicating that at lower frequencies, past tumor-immune interactions have a greater impact. At $\alpha = 1$, the response becomes narrower and instantaneous, and the effects of memory disappear in classical models.

9.2. Clinical relevance and validation

The fractional-order hybrid model presented in this study provides qualitative insights into NSCLC progression and therapeutic response. The simulation trajectories - including slower tumor regression, prolonged immune activation, and relapse patterns - reflect clinical phenomena commonly reported in patient studies. For example, model-predicted delayed immune responses and immune exhaustion are more consistent with CD8⁺ T lymphocyte counts observed in biopsy-based immunological assays, and fractional tumor decay mirrors volumetric tumor dynamics measured with imaging modalities such as CT and MRI.

Although the present work emphasizes theoretical formulation and qualitative validation, quantitative comparison with real-world NSCLC datasets remains important for future directions. Specifically, calibration of model parameters against imaging-derived tumor volume dynamics, immune cell kinetics from flow cytometry, and survival outcomes from clinical trials would strengthen translational applicability. Such integration would enable patient-specific parameterization, thereby enhancing the framework's predictive power for personalized treatment planning.

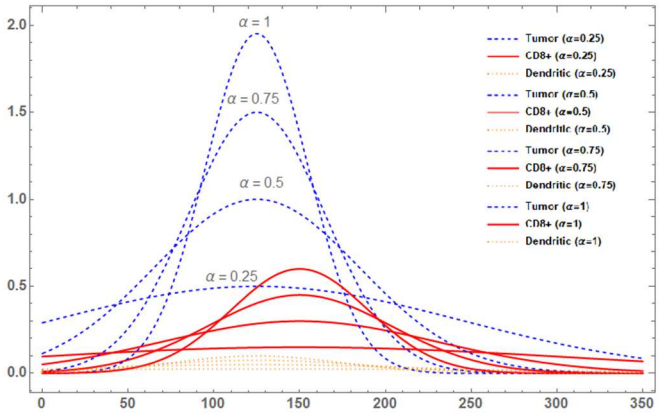

Fig. 2. Fractional-order dynamics of tumor cells, CD8⁺ T cells, and dendritic cells for $\alpha = 0.25, 0.5, 0.75, 1$.

By embedding hereditary immune memory into tumor–immune–therapy interactions, the proposed fractional-order model not only advances mathematical oncology but also establishes a foundation for bridging computational predictions with clinical data. This translational pathway underscores the potential of fractional dynamics to inform individualized therapeutic strategies in NSCLC.

9.3. Biological interpretation

The simulations, based on fractional-order models compared to integer-order models, show the following characteristics: slower tumor decay, longer immune activation, and delayed system equilibria. These findings emphasize the need to consider the effects of memory in cancer modeling, as it offers a more realistic interpretation of tumor survival, immune fatigue, and long-term monitoring.

10. Fractional-Order Computational Dynamics and Biomechanical Control Framework for NSCLC Systems

The section develops a hybrid treatment model of NSCLC by combining fractional-order tumor-immune dynamics, using the He complex transform, with discrete clinical treatments (surgical cytoreduction and periodic chemotherapy).

10.1. Hybrid system formulation

The proposed framework is an impulsive differential system in which fractional-order differential equations govern continuous tumor-immune dynamics and discrete therapeutic interventions are modeled as impulsive events. Surgery is represented as a one-time impulsive reduction in tumor cell population at a specified time instant, and chemotherapy is incorporated as a sequence of periodic impulses that perturb both malignant and immune cell compartments.

This formulation allows the system to switch between continuous fractional dynamics and discrete perturbations, thereby capturing the hybrid nature of clinical treatment regimens. The impulsive system framework ensures that therapeutic events are explicitly embedded into the model equations, enabling rigorous analysis of stability, equilibrium, and long-term outcomes under combined continuous and discrete dynamics. Future extensions could explore event-triggered control formulations in which interventions are activated based on tumor thresholds or immune exhaustion, further enhancing clinical realism.

10.2. Model and fractional transform

Discrete treatment events in clinical times

- $T^+ = (1-\sigma_C)T^-$ [T is reduced by the chemo efficacy factor σ_C (i.e. $\sigma_C = 99\%$ cytoreduction)]
- $C^+ = (1-\chi_C)C^-$ [C is reduced by χ_C, chemo-induced lymphopenia/immunosuppression]
- $D^+ = (1-\delta_C)D^-$ [D is reduced by δ_C, the chemo impact on APCs]

If $T^-, C^-, D^- \geq 0$ then $T^+, C^+, D^+ \geq 0$. Since each factor $1-\sigma_C, 1-\chi_C, 1-\delta_C \in (0,1)$, for any positive state, each component strictly decreases at $T^+ < T^-, C^+ < C^-, D^+ < D^-$.

In Fig. 3(a), the number of tumor cells decreases steadily across all fractional orders from day 1. The rate of decline, however, depends strongly on the fractional order α. For lower values $\alpha = 0.7$ (blue, dashed), tumor suppression is faster, and the curve remains lower throughout the simulation.

In the case of intermediate $\alpha = 0.85$, the decrease is slight yet effective, whereas in the case of $\alpha = 1.0$, i.e., the classical case, the tumor cells remain at higher levels for longer before levelling off. This proves that fractional dynamics increase tumor persistence relative to integer-order equations, reflecting hereditary effects in tumor growth and immune suppression.

The dynamics of CD8⁺ T cells are presented in Fig. 3(b). During the initial 30 days, there is a progressive increase in CD8⁺ T cells, regardless of α. Beyond day 30, the curves separate because increasing α values result in greater immune activation, with plateaus observed in CD8⁺ T cells. Lower values of α, on the contrary, result in weaker and more persistent responses, which is compatible with immune exhaustion and delayed surveillance. At approximately 150 days, all curves level off, although the extent of the immune response is still α dependent.

Based on Fig. 3(c), the dendritic cell values decrease with time regardless of the α values. During the initial 70 days, the curves are similar. Subsequently, the curves diverge: the larger the α values, the slower the reduction; the smaller the α values, the more rapid the reduction they cause. This indicates the spread of dendritic activation (a time-based process), in which the antigen presentation process traps memory effects.

Contrary to classical integer-order models, these curves demonstrate memory effects and how fractional dynamics can modify tumor suppression, immune activation, and dendritic cell persistence. This better accounts for clinical phenomena such as immune exhaustion, relapse, and long-term surveillance, aiding the design of treatment strategies with delayed or extended immune responses.

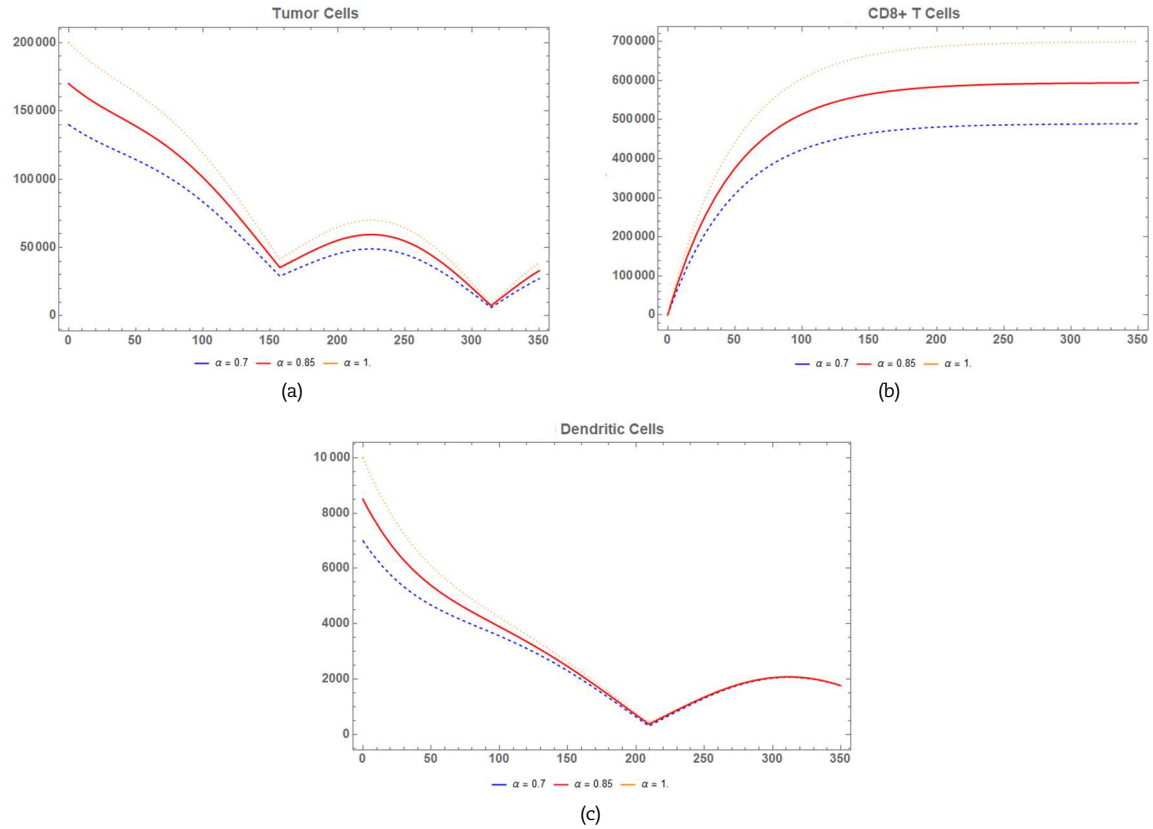

Fig. 3. (a) Fractional-order behavior of Tumor cells under computational control dynamics and biomechanical regulation, (b) Fractional-order behavior of CD8⁺ T cells under computational control dynamics and biomechanical regulation, (c) Fractional-order behavior of dendritic cells under computational control dynamics and biomechanical regulation.

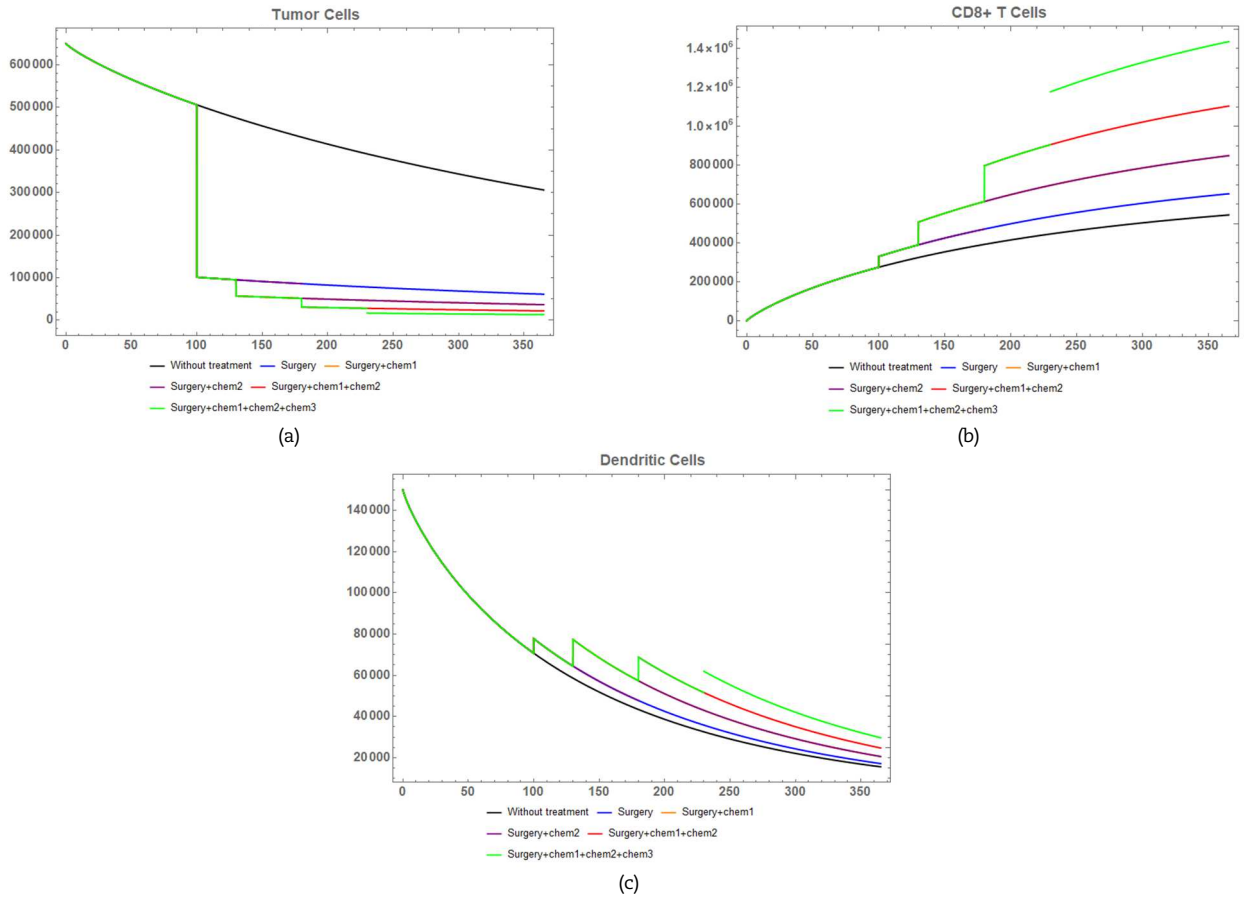

Fig. 4. (a) Fractional-order dynamics of tumor cells for various treatment methods, (b) Fractional-order dynamics of CD8⁺ T cells for various treatment methods, (c) Fractional-order dynamics of dendritic cells for various treatment methods.

Figure 4(a) shows that tumor cell growth is steady over the period from day 1 to day 100 in all the treatment conditions. Surgery eliminates about 80-95 percent of tumor cells at day 100, giving a sharp fall. Unless chemotherapy is done after the surgery, the tumor cells start growing and become erratic once again. At day 130, when the initial amount of chemotherapy is administered, the tumor cells are further suppressed, although the rebounds are slower than in a classical model because of fractional dynamics $\alpha = 0.85$. A second dose at day 180 is more effective than the first dose at reducing tumor cells, and two sequential doses (chem1 + chem2) maintain a low level of tumor cells until day 250. The most complex treatment (surgery + chem1 + chem2 + chem3) keeps tumor cells nearly at zero throughout the simulation, demonstrating the amplifying effect of multi-agent therapy.

Figure 4(b) shows that, in the absence of treatment, the number of $CD8^+$ T cells increases gradually due to the stimulation of immune activation by dendritic cells. On day 100, $CD8^+$ T cells decrease significantly after surgery, due to decreased dendritic cell antigen presentation. Unless chemotherapy is given, the $CD8^+$ T cells will heal and revert once more. After the initial dose of chemotherapy, the number of $CD8^+$T cells decreases further as chemotherapy targets the tumor and rapidly growing immune cells. Beyond day 225, with no further chemotherapy, $CD8^+$ T cells start to increase once again. Immunological activation of patients who received the second dose after a missed first dose is weaker than the patients who received the first dose. The combination of two doses (chem1 + chem2) inhibits $CD8^+$T cells more potently, leading to later recovery. The three doses (chem1 + chem2 + chem3) are effective in maintaining $CD8^+$T cell depletion until day 350, which manifests long-term immune suppression on a fractional basis.

Figure 4(c) shows dendritic cells deteriorate until day 100. To some extent, surgery can mitigate this degradation, but in the absence of chemotherapy, cell depletion continues. The initial dose of chemotherapy, due to its indiscriminate nature, eliminates more dendritic cells. Postoperative dendritic cell levels are lower in the second dose than in the first dose. Two successive doses (chem1 + chem2) more effectively suppress dendritic cells, and the process is followed by recovery. The three doses (chem1 + chem2 + chem3) can maintain dendritic cell reduction during the simulation period and demonstrate long-term suppression. With time, fractional dynamics increase dendritic activation, making it smoother with declines and delayed rebounds compared to integer-order models. These curves illustrate that the introduction of memory effects due to the use of fractional-order models with $\alpha = 0.85$ has changed tumor suppression, immune activation, and dendritic persistence in classical integer-order models. The graph illustrates that surgery paired with several cycles of chemotherapy gradually enhances tumor control and weakens immune cells. The given balance helps emphasize the role of fractional dynamics in estimating realistic treatment results and designing therapies.

In Fig. 5(a), tumor cell dynamics reveal that integer-order models predict a sharp decline once immune pressure or treatment is applied, and fractional-order models show slower suppression with lingering tumor presence. This difference highlights the role of memory effects, where past tumor states influence current behavior, making relapse or prolonged survival more realistic. Figure 5(b) compares $CD8^+$ T cell responses. In the integer-order case, immune activation is rapid and intense but short-lived, peaking quickly before declining. The fractional-order model, however, produces weaker but longer-lasting activation, with delayed peaks and signs of immune exhaustion. This sustained-but-lower-intensity response reflects the hereditary nature of immune surveillance. Figure 5(c) illustrates dendritic cell dynamics. Integer-order models depict sharp, narrow activation peaks that rise and fall abruptly.

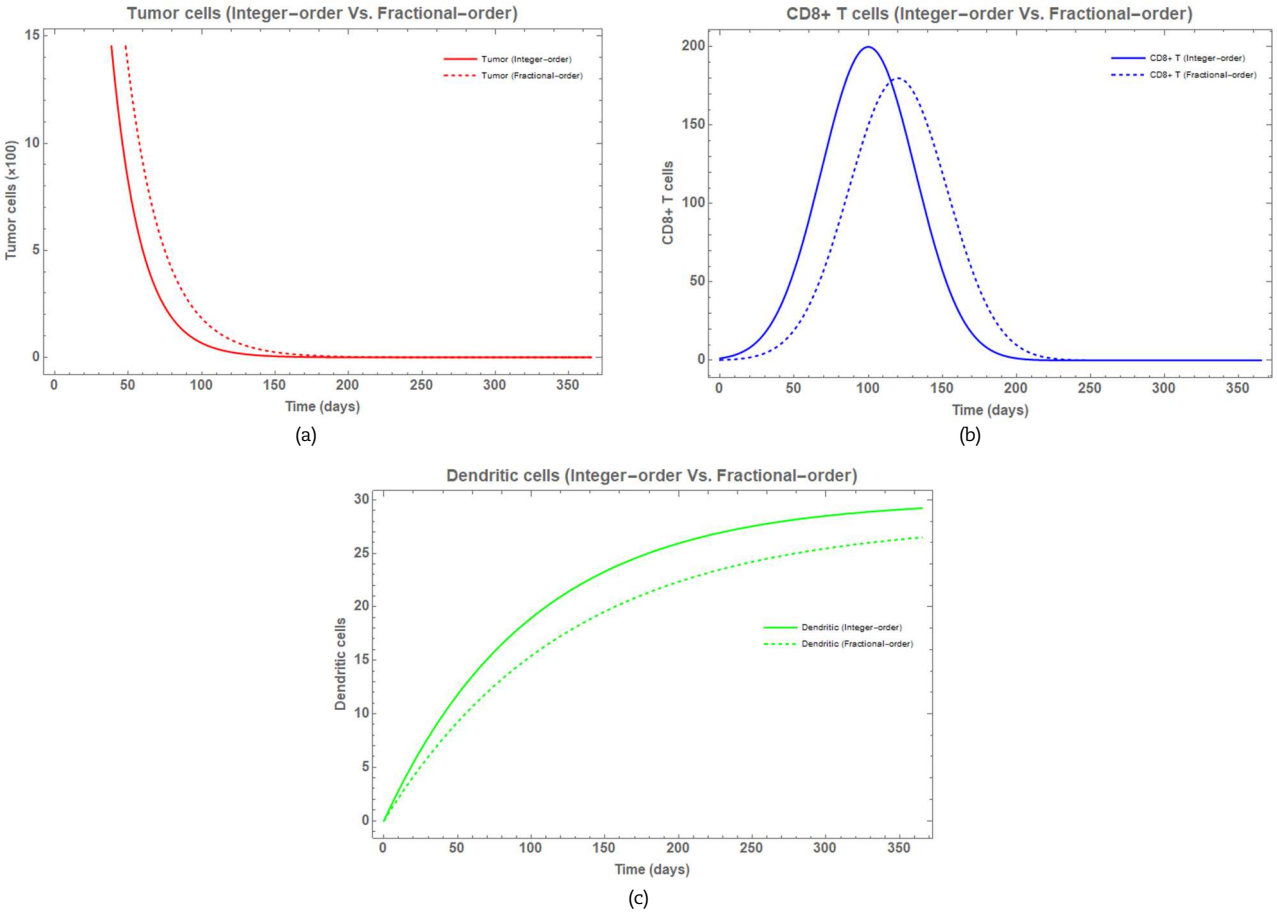

Fig. 5. (a) Comparative dynamics of tumor cells under integer-order and fractional-order models, (b) Comparative dynamics of $CD8^+$ T cells under integer-order and fractional-order models, (c) Comparative dynamics of dendritic cells under integer-order and fractional-order models.

In contrast, fractional-order models produce smoother, more diffuse activation curves, where past tumor–immune interactions extend dendritic activity and delay recovery. This captures the memory-driven modulation of antigen presentation. Overall, Figs. 5(a) to 5(c) show that integer-order models oversimplify tumor-immune dynamics, leading to abrupt transitions, and fractional-order models capture memory effects that produce slower, prolonged, and biologically realistic responses.

11. Conclusion

The non-small-cell lung cancer (NSCLC) fractional-order hybrid model in this paper shows that the effects on memory and hereditary dynamics can dramatically change tumor-immunity-therapy interactions. The model incorporates computational control dynamics and biomechanical regulation as discrete events for a continuous immune-tumor model, including immune exhaustion, delayed surveillance, and tumor relapse. The equilibrium and stability analysis observes critical numbers, such as the basic reproduction number, which determines whether the tumor persists or is eliminated. Numerical simulations demonstrate that fractional dynamics have slower tumor decay, longer immune responses, and a slower equilibrium than classical integer-order models, therefore providing a more biologically realistic model of cancer progression and treatment responses. The suggested hybrid fractional-order model provides various potential research directions. A notable extension is individualized treatment planning, in which personalized parameters are used to create tailored regimens, improving prognosis and reducing side effects. The other pathway is inserting immunotherapy (such as checkpoint inhibitors and CAR-T cells) into the fractional system to assess its long-term effects in the context of hereditary immune interactions. Thus, the framework paves the way for the development of mathematical oncology, providing a solid platform for developing adaptive and memory-responsive approaches to NSCLC treatment. The proposed framework also contributes to recent advances in computational biomechanics and nonlinear dynamical system analysis, thereby strengthening its applicability within modern computational mathematics and engineering research.

Author Contributions

S.A. Ambhore conceptualized the study, developed the methodology, performed the formal analysis and investigation, and prepared the original draft of the manuscript. N.K. Lamba contributed to the review and editing of the manuscript, acquired funding, provided resources, and supervised the project. The manuscript was written through the contributions of all authors. All authors discussed the results, reviewed, and approved the final version of the manuscript.

Acknowledgments

The authors would like to express their sincere gratitude to the Editor-in-Chief and the anonymous reviewers for their constructive comments and valuable suggestions, which have significantly improved the quality and presentation of this manuscript.

Conflict of Interest

The authors declared no potential conflicts of interest concerning the research, authorship, and publication of this article.

Funding

The author, N.K. Lamba, gratefully acknowledges the Research and Development Cell of R.T.M. Nagpur University for financial support under the URPS (Letter No. RTMNU/RDC/2026/508) and for the university's ongoing encouragement.

Data Availability Statements

The datasets generated and/or analyzed during the current study are available from the corresponding author on reasonable request.

References

[1] Sung, H., Ferlay, J., Siegel, R. L., Laversanne, M., Soerjomataram, I., Jemal, A., Bray, F., Global cancer statistics 2020: GLOBOCAN estimates of incidence and mortality worldwide for 36 cancers in 185 countries, *CA: A Cancer Journal for Clinicians*, 71(3), 2021, 209–249.
[2] Hirsch, F. R., Scagliotti, G. V., Mulshine, J. L., Kwon, R., Curran, W. J., Wu, Y. L., Paz-Ares, L., Lung cancer: Current therapies and new targeted treatments, *The Lancet*, 389(10066), 2017, 299–311.
[3] de Pillis, L. G., Radunskaya, A. E., Wiseman, C. L., A validated mathematical model of cell-mediated immune response to tumor growth, *Cancer Research*, 65(17), 2005, 7950–7958.
[4] Ullah, A., Mallick, S., A fractional-order mathematical model for the treatment of non-small-cell lung cancer using surgery and chemotherapy, *Alexandria Engineering Journal*, 72, 2023, 1–15.
[5] Magin, R. L., Fractional calculus models of complex dynamics in biological tissues, *Computers & Mathematics with Applications*, 59(5), 2010, 1586–1593.
[6] Varghese, V., Bhoyar, S., Nisar, K. S., Analysis of fractional-order model of COVID-19 pandemics with a nonlinear incidence rate, *Innovative Biosystems and Bioengineering*, 4(3), 2020, 160–167.
[7] Dunn, G. P., Old, L. J., Schreiber, R. D., The immunobiology of cancer immunosurveillance and immunoediting, *Immunity*, 21(2), 2004, 137–148.
[8] Palucka, K., Banchereau, J., Cancer immunotherapy via dendritic cells, *Nature Reviews Cancer*, 12(4), 2012, 265–277.
[9] Gandhi, L., Rodríguez-Abreu, D., Gadgeel, S., Esteban, E., Felip, E., De Angelis, F., Garassino, M. C., Pembrolizumab plus chemotherapy in metastatic non–small-cell lung cancer, *New England Journal of Medicine*, 378(22), 2018, 2078–2092.
[10] Li, Z. B., He, J. H., Fractional complex transform for fractional differential equations, *Mathematical and Computational Applications*, 15(5), 2010, 970–973.
[11] Sulimanov, R., Koshelev, K., Makarov, V., Mezentsev, A., Durymanov, M., Ismail, L., Laskov, I., Mathematical modeling of non-small-cell lung cancer biology through the experimental data on cell composition and growth of patient-derived organoids, *Life*, 13(11), 2023, 2228.
[12] He, J., Elgazery, N. S., Abd Elazem, N. Y., Gold nanoparticles' morphology affects blood flow near a wavy biological tissue wall: An application for cancer therapy, *Journal of Applied and Computational Mechanics*, 10(2), 2024, 342–356.
[13] Wan Azmi, W. F., Mohamad, A. Q., Jiann, L. Y., Shafie, S., Mathematical modelling of MHD blood flow with gold nanoparticles in slip small arteries, *Journal of Applied and Computational Mechanics*, 10(1), 2024, 125–139.
[14] Almuneef, A., Abbas, I., El-Bary, A. A., Alqahtani, Z., The impacts of Atangana–Baleanu fractional derivative in biological tissues during thermotherapy, *Journal of Applied and Computational Mechanics*, 12(1), 2026, 51–59.

[15] Alotaibi, H., Baleanu, D., El-Sayed, A., Fractional computational biomechanics modeling for nonlinear tumor–immune interaction systems, *Journal of Computational and Applied Mathematics*, 442, 2025, 115732.
[16] Kumar, S., Naik, P. A., Shah, K., Dynamical analysis of fractional-order cancer–immune interaction models with memory effects, *Chaos, Solitons & Fractals*, 188, 2025, 115432.
[17] Rahman, M., Farman, M., Ahmad, A., Computational dynamics of nonlinear biomechanical cancer systems using fractional calculus, *Computer Methods and Programs in Biomedicine*, 267, 2026, 108214.
[18] Zhang, Y., Liu, X., Baleanu, D., Fractional-order computational modeling of biological dynamical systems with tumor–immune interactions, *Applied Mathematical Modelling*, 142, 2026, 114998.
[19] Singh, V., Kumari, N., Srivastava, S. K., Computational biomechanics and fractional-order oncology dynamics with immune memory effects, *International Journal of Dynamics and Control*, 14(6), 2026, 455–472.
[20] Alabedalhadi, M., Salameh, W., Al-Omari, S., Karaca, Y., Al-Smadi, M., Baleanu, D., Momani, S., Analysis of a fractional order model for the interaction between growth and crowding of tumor stem cells via Caputo fractional derivatives, *Fractals*, 38, 2026, 2640012.
[21] Singh, V., Kumari, N., Sinha, S., Srivastava, S. K., A fractional-order tumor–immune system model with combined vitamin and chemotherapy: Analysis, stability, and control insights, *International Journal of Dynamics and Control*, 14(4), 2026, 116.
[22] Alchikh, R., Fayyad-Kazan, M., Khuri, S. A., A semi-analytical approach for solving a fractional-order mathematical model of skin cell damage and repair driven by environmental pollutants, *Scientific Reports*, 16, 2026, 6399.
[23] Naik, P. A., Kulachi, M. O., Ahmad, A., Farman, M., Iqbal, F., Taimoor, M., Huang, Z., Modeling different strategies towards control of lung cancer: Leveraging early detection and anti-cancer cell measures, *Computer Methods in Biomechanics and Biomedical Engineering*, 29(3), 2026, 603–617.
[24] Huang, D., Liu, M., Chen, T., Wang, W., Xiao, D., He, H., Rao, D., Tissue-derived single vesicle membrane proteomics reveals potential biomarkers for diagnosis and prognosis of non-small cell lung cancer, *Biomedical Signal Processing and Control*, 115, 2026, 109374.
[25] Liu, F. J., Li, Z. B., Zhang, S., Liu, H. Y., He's fractional derivative for heat conduction in a fractal medium arising in silkworm cocoon hierarchy, *Thermal Science*, 19(4), 2015, 1155–1159.

ORCID iD

Shubham Ashok Ambhore https://orcid.org/0009-0006-6420-1401
Navneet Kumar Lamba https://orcid.org/0000-0002-6283-1681

© 2026 Shahid Chamran University of Ahvaz, Ahvaz, Iran. This article is an open access article distributed under the terms and conditions of the Creative Commons Attribution-NonCommercial 4.0 International (CC BY-NC 4.0 license) (http://creativecommons.org/licenses/by-nc/4.0/).

How to cite this article: Ambhore S.A., Lamba N.K. Dynamic Fractional-Order Computational Modeling of Lung Cancer: A Hybrid Biomechanical–Therapy Framework, *J. Appl. Comput. Mech.*, 12(4), 2026, 1650-1666.
https://doi.org/10.22055/jacm.2026.49360.5917

Publisher's Note Shahid Chamran University of Ahvaz remains neutral with regard to jurisdictional claims in published maps and institutional affiliations.